THE JOURNAL OF PHYSICAL CHEMISTRY Letters

Letter

Cite This: J. Phys. Chem. Lett. 2019, 10, 2554−2560

pubs.acs.org/JPCL

Hard BN Clathrate Superconductors

Xue Li,[†,▽] Xue Yong,[‡,▽] Min Wu,[§] Siyu Lu,[*,‡] Hanyu Liu,[*,†] Sheng Meng,[∥] John S. Tse,[⊥] and Yinwei Li[*,#]

[†]State Key Laboratory of Superhard Materials & Innovation Center for Computational Physics Methods and Software, College of Physics, Jilin University, Changchun, Jilin 130012, China

[‡]College of Chemistry and Molecular Engineering, Zhengzhou University, 100 Kexue Road, Zhengzhou 450001, China

[§]College of Materials Science and Engineering, Zhejiang University of Technology, Hangzhou 310014, China

[∥]Institute of Physics, Chinese Academy of Sciences, Beijing 100190, P. R. China

[⊥]Department of Physics and Engineering Physics, University of Saskatchewan, Saskatoon, Saskatchewan S7N 5E2, Canada

[#]Laboratory of Quantum Materials Design and Application, School of Physics and Electronic Engineering, Jiangsu Normal University, Xuzhou 221116, China

Supporting Information

ABSTRACT: The search for hard superconductive materials has attracted a great deal of attention due to their fundamentally interesting properties and potentially practical applications. Here we predict a new class of materials based on sodalite-like BN frameworks, $X(BN)_6$, where X = Al, Si, Cl, *etc*. Our simulations reveal that these materials could achieve high superconducting critical temperatures (T_c) and high hardness. Electron−phonon calculations indicate that T_c of these compounds varies with the doping element. For example, the superconducting T_c of sodalite-like $Al(BN)_6$ is predicted to reach ∼47 K, which is higher than that in the renowned MgB_2 (39 K). This phase and a series of other sodalite-based superconductors are predicted to be metastable phases but are dynamically stable as well. These doped sodalite-based structures are likely to become recoverable as potentially useful superconductors with high hardness. Our current results present a new strategy for searching for hard high-T_c materials.

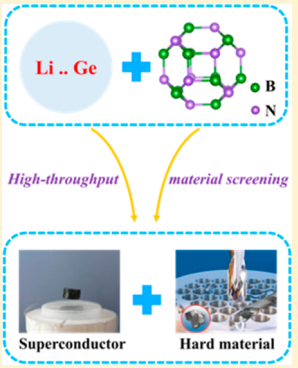

Open-structure clathrate compounds, in particular those of Group IV elements, have received significant attention owing to their potential superconductivity, low thermal conductivity, and high hardness. Although Si, Ge, and Sn clathrates have been synthesized, many studies have sought carbon-based clathrates,[1−4] which have been predicted to be superconducting with high critical temperatures (T_c) and easily dopable with metals. BN is isoelectronic with carbon and forms analogues of various carbon structures, for example *h*-BN,[5] *r*-BN,[6] *c*-BN,[7] *w*-BN,[8] amorphous BN,[9] BN nanotubes,[10] and BN nanomesh.[11] However, unlike Group IV clathrates,[1,2,12,13] few BN clathrates, in particular doped clathrates, have been reported. BN clathrates could exploit the unique electron deficiency of B atoms and electron-rich N atoms to allow both *p*- and *n*-type doping with light, nontoxic elements, paving the road for environmentally friendly multifunctional clathrates.

B and N could form strong covalent compounds[14−17] at high temperature and high pressure. Given the sp^3 bonding that forms in BN frameworks, the covalent states could interact with phonons, and the enhanced electron−phonon coupling (EPC) could produce superconductivity. Several high-pressure-induced BN polymorphs[18] have been recovered under ambient conditions. Therefore, the high-pressure synthesis of BN compounds may provide a way for searching for high-T_c superconductors with potential industrial applications. This finding has motivated our investigation of BN clathrates.

In our previous work,[19] we reported the first cubic sodalite BN structure (space group symmetry *Pm*-3*n*) that is stable under ambient conditions, because it has a formation enthalpy that is more negative than other BN structures. The structure, identical to that of *c*-BN, comprised planar B_3N_3 hexagonal faces with B−N bond lengths of 1.57 Å. In the present study, we propose a range of new BN clathrates via doping the sodalite BN framework with different elements. Electron−phonon calculations based on BCS theory[20] imply that these compounds are superconductors with high T_c above 39 K at ambient pressure. Electron charge transfer in the phonon dispersion may be responsible for such high T_c. These materials may also possess high hardness. We anticipate that high-temperature and high-pressure techniques may be helpful to form doped BN sodalite phases that are metastable at ambient conditions. This work may aid the study of superconducting behavior in conventional superconductors and the practical applications of superconductors.

Received: March 4, 2019
Accepted: May 3, 2019
Published: May 3, 2019

DOI: 10.1021/acs.jpclett.9b00619
J. Phys. Chem. Lett. 2019, 10, 2554−2560

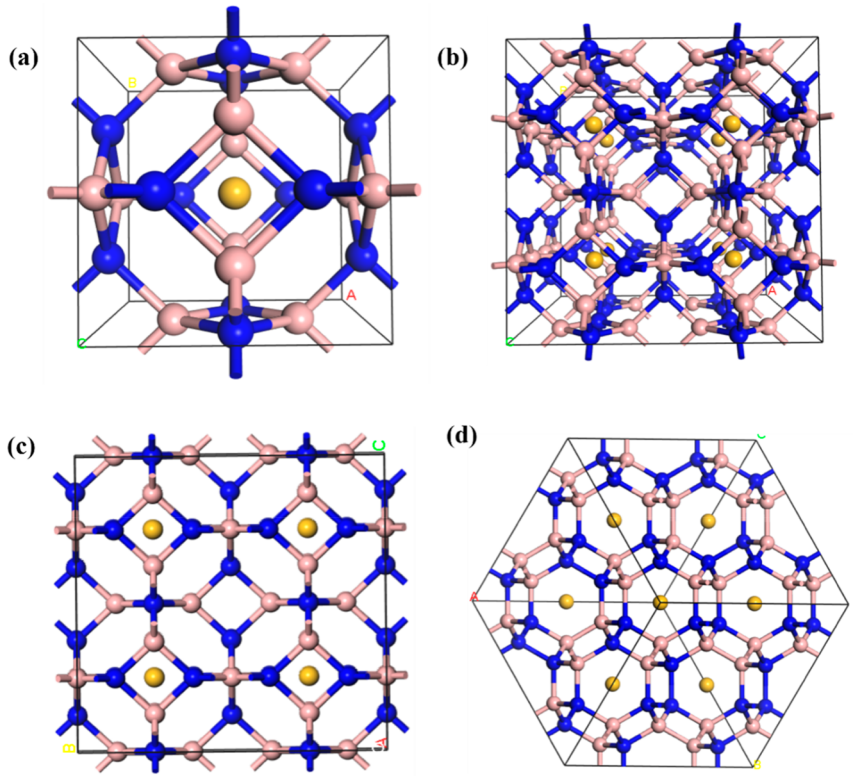

Figure 1. Crystal structures of $Si(BN)_6$: (a) is the unit cell, and (b), (c), and (d) are the supercell viewed along different directions. Yellow, pink, and blue spheres represent Si, B, and N atoms.

The cubic sodalite BN framework is an ideal hard material, and suitably doping is expected to result in superconductivity. This is in contrast to most superconductors (e.g., hydrides), which are rather soft, and is likely to be recovered to ambient conditions. In order to achieve high superhardness and superconductivity, we systematically examine sodalite-like high-lattice-symmetry BN frameworks doped with light elements at ambient pressure. We propose a series of dynamically stable $X(BN)_6$ (X = B, C, N, O, F, Al, Si, P, S, Cl, Ga, Ge) compounds with the same basic structure. These new compounds are plausible hard superconducting materials, since these predicted structures possess three-dimensional B−N covalent bonds.

An example of our compounds, $Si(BN)_6$, has a Si atom inserted in the center of each sodalite BN cage. After full optimization of the lattice and atomic positions, $Si(BN)_6$ has a cubic crystal structure (space group *Pm*-3) with lattice parameter $a = b = c = 4.59$ Å (Figure 1). The structure consists of planar B_3N_3 hexagonal faces with B−N bond lengths of 1.63 Å and planar B_2N_2 rhombic faces with B−N bond lengths of 1.61 Å. Eight hexagons and six rhombuses in the unit cell are linked to each other by sharing B−N edges, thereby forming B_6N_6 sodalite-like cages. The B and N atoms form a rhombohedral structure with both B−N−B and N−B−N angles of either around 90° or 120°. Similarly, the other materials also have cubic crystal structures with the same space group and similar lattice constants, indicating that the choice of doping element has almost unaffected the structures. However, doping itself has a distinct effect on the bond lengths (Figure S5). The B−N bonds in pure $(BN)_6$ cages are around 1.571 Å, whereas in the doped compounds they range from 1.615 Å in $Si(BN)_6$ to 1.627 Å in $Al(BN)_6$.

We computed the band structures and electron localization functions (ELFs) to explore the changes in the electronic properties of the doped sodalite BN. Figure 2 presents selected results for $Al(BN)_6$, $Si(BN)_6$, and $Cl(BN)_6$. The ELFs indicate strong covalent bonding between the B and N atoms but weak interactions between the dopants and the BN cage. Density functional theory calculations indicate that the whole doped structures are metallic phases. Orbital resolved band structures show that the occupied bands close to the Fermi level of all three doped systems are mainly derived from the *p* orbital of the dopant, whereas the unoccupied bands are mainly derived from the *p* orbital of B. Interestingly, comparison with the band structure of the empty $(BN)_6$ cage shows that the dopants contribute slightly to the energy levels around the Fermi level. In addition, all band structures show steep flat bands crossing the Fermi energy. The sodalite BN cage is a semiconductor with a wide indirect band gap of 4.32 eV. The band structures of the doped and undoped systems are almost identical, but doping shifts the Fermi level. Shifts of 4.1 eV in $Al(BN)_6$ and 2.18 eV in $Si(BN)_6$ move the Fermi level to the conduction band, and the shift of 1.5 eV in $Cl(BN)_6$ puts it in the valence band. The transition of the undoped semiconducting $(BN)_6$ cage to a doped metallic system is due to electron charge transfer between the dopant and the B and N atoms. Bader charge analysis indicates that Si and Al donate 0.53*e* and 1*e* to the BN cage, respectively, whereas Cl obtains 0.28*e* from the $(BN)_6$ cage as shown in Table 1. Cl acts as a *p*-type dopant, whereas Si and Al are *n*-type dopants. Therefore, the combination of electron-deficient B and electron-rich N allows doping by both *n*- and *p*-type light elements. The addition or loss of electrons leads to partial occupancy of the degenerate bands in $(BN)_6$, as shown in the band structures, resulting in the metallic character of the doped systems. Partial

DOI: 10.1021/acs.jpclett.9b00619
J. Phys. Chem. Lett. 2019, 10, 2554−2560

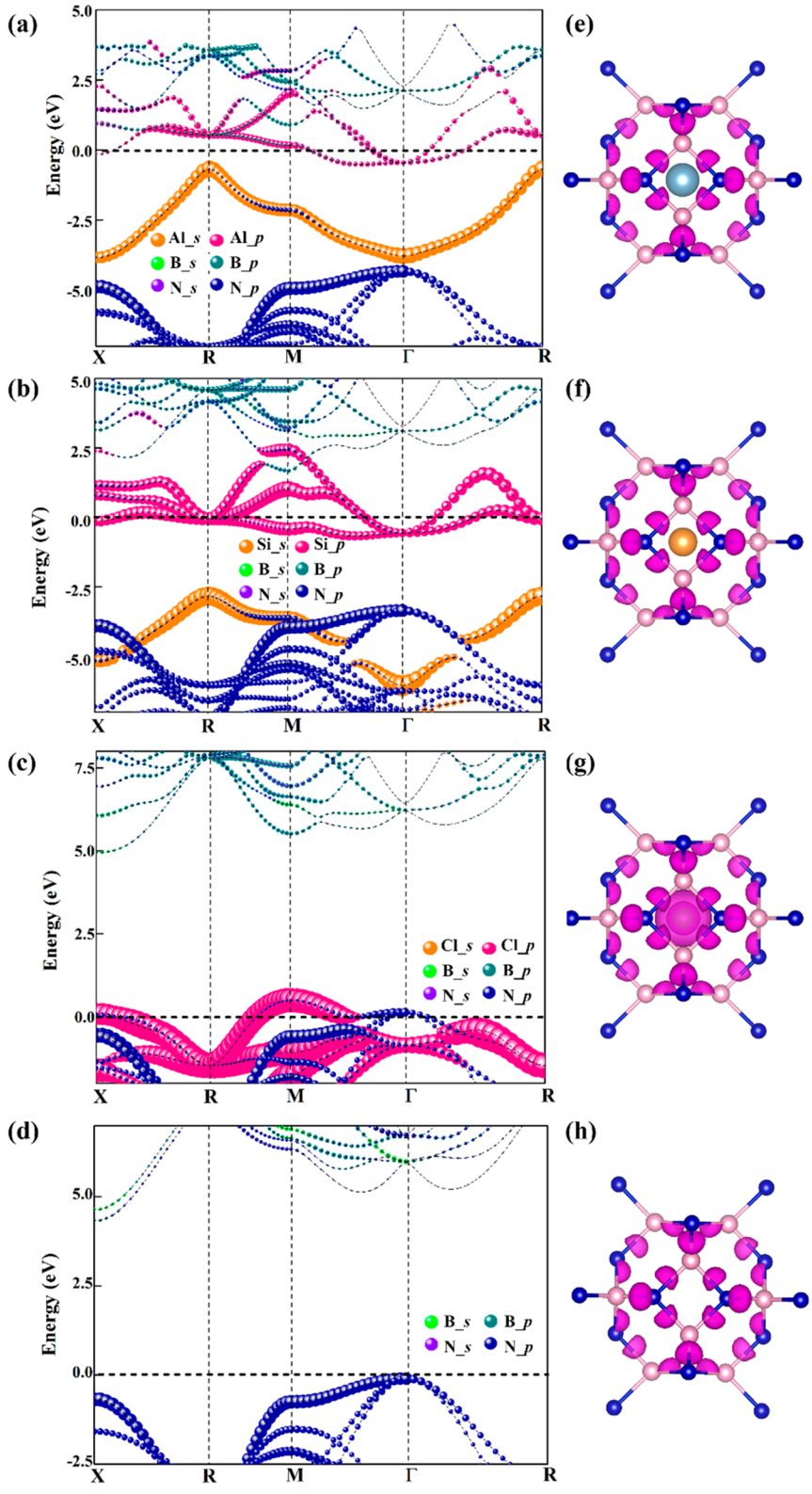

Figure 2. Electronic properties: Band structures of (a) $Al(BN)_6$, (b) $Si(BN)_6$, (c) $Cl(BN)_6$, and (d) $(BN)_6$. The horizontal magenta dotted lines indicate the Fermi level. Electron localization functions of (e) $Al(BN)_6$, (f) $Si(BN)_6$, (g) $Cl(BN)_6$, and (h) $(BN)_6$. Yellow, pink, and blue spheres represent Al/Si/Cl, B, and N atoms.

occupancy of degenerate orbitals results in an orbital degeneracy, which is likely subject to Jahn−Teller (JT) distortion.[21] The JT effect involves coupling between the electronic and nuclear degrees of freedom, which leads to distortions in the geometric structure to alleviate the orbital degeneracy. If the distortion is dynamic, JT vibration, which is a strong EPC process, will lead to superconductivity. The same mechanism has been attributed as the superconductivity of B-doped diamond.

DOI: 10.1021/acs.jpclett.9b00619
J. Phys. Chem. Lett. 2019, 10, 2554−2560

Table 1. Calculated Bader Charge Transfer between Doped Elements and B/N in $Al(BN)_6$, $Si(BN)_6$, and $Cl(BN)_6$

	doped element (Al/Si/Cl)	B	N
$Al(BN)_6$	1.00	2.04	−2.2
$Si(BN)_6$	0.53	2.06	−2.15
$Cl(BN)_6$	−0.28	2.14	−2.09

We confirmed the lattice dynamics of the doped systems with the help of phonon calculations. We have simulated the phonon spectrum and the projected phonon density of states as shown in Figure 3 and Figures S1 and S2. The absence of imaginary frequencies in the whole Brillouin zone (BZ) indicates that those doped structures are dynamically stable. The whole phonon spectrum of the doped system is shifted to a lower frequency relative to undoped $(BN)_6$. A heavier dopant yields lower-energy vibrations that help mediate EPC. B and N dominate the vibrational modes with frequencies above 250 cm^{-1}, as the doped elements dominate the modes below 250 cm^{-1}. For example, the $Al(BN)_6$ doped system has two separate phonon band regions. The gap between the acoustic and optical phonon branches indicates that $Al(BN)_6$ has ionic character. In contrast, band crossings between the two branches are observed for $Si(BN)_6$ and $Cl(BN)_6$. Thus, they show weak EPC interactions.

We investigated the potential superconductivity of our predicted structures using the McMillan equation based on BCS theory. We derive T_c from the spectral function, $\alpha^2F(\omega)$, using a typical Coulomb pseudopotential of $\mu^* = 0.1$.

$$T_c = \frac{\hbar\omega_{\log}}{1.2}\exp\left[\frac{1.04(1+\lambda)}{\lambda-\mu^*-0.62\lambda\mu^*}\right] \quad (1)$$

Here, λ is the first reciprocal moment of the spectral function

$$\lambda = 2\int_0^\infty \frac{\alpha^2F(\omega)}{\omega}d\omega \approx \sum_{qj}\lambda_{qj}\omega(\boldsymbol{q}) \quad (2)$$

where $\omega(\boldsymbol{q})$ is the weight (weights account for the symmetries of the BZ) of a $\boldsymbol{q}$ point in the first BZ, and the EPC spectral function, $\alpha^2F(\omega)$, is expressed in terms of the phonon line width, γ_{qj}, arising from EPC.

$$\alpha^2F(\omega) = \frac{1}{2\pi N_f}\sum_{qj}\frac{\gamma_{qj}}{\omega_{qj}}\delta(\omega-\omega_{qj})\omega(q) \quad (3)$$

Here, N_f is the electronic density of electron states at the Fermi level. The line width, γ_{qj}, of phonon mode j at wave vector $\boldsymbol{q}$ arising from EPC is

$$\gamma_{qj} = 2\pi\omega_{qj}\sum_{nm}\int\frac{d^3k}{\Omega_{BZ}}\left|g^j_{kn,k+qm}\right|^2\times\delta(\xi_{kn}-\xi_F)\times\delta(\xi_{k+qm}-\xi_F) \quad (4)$$

where the sum is over the first BZ, Ω_{BZ} is the volume of the BZ, and ξ_{kn} denotes the energies of bands (measured with respect to the Fermi ξ_F level) at point K. Here, $g^j_{kn,k+qm}$ is the electron−phonon matrix element for scattering from an electron in band n at wave vector k to band m at wave vector $\boldsymbol{k}+\boldsymbol{q}$ via a phonon with wave vector $\boldsymbol{q}$.

Furthermore, we computed the EPC constants of $X(BN)_6$ (X = B, C, N, O, F, Al, Si, P, S, Cl, Ga, Ge) at ambient pressure. The specific EPC integration, $\lambda(\omega_{\log})$, and transition temperature are listed in Figure 4 and Table S2. Doping with

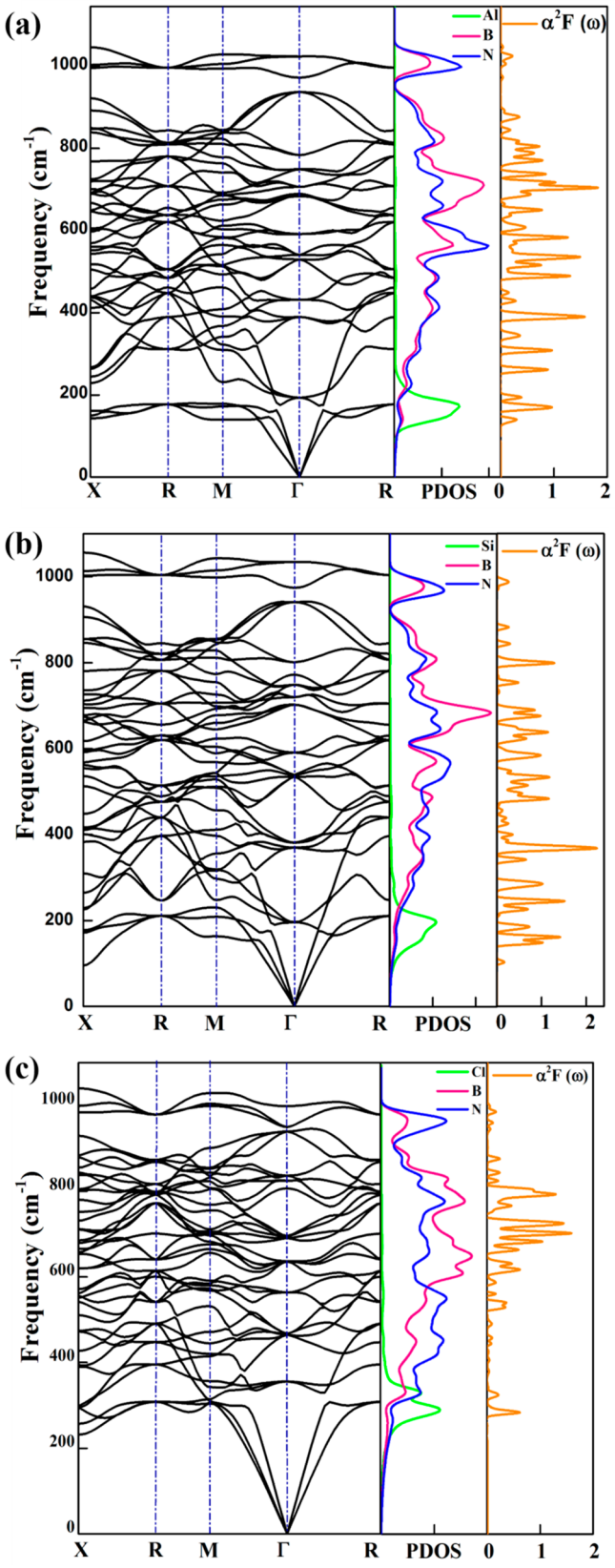

Figure 3. Phonon properties: Phonon dispersions and projected phonon density of states (PHDOS) of (a) $Al(BN)_6$, (b) $Si(BN)_6$, and (c) $Cl(BN)_6$.

Al produces a good superconductor with T_c = 47 K, which is higher than that of MgB_2 (39 K) at ambient pressure. Al has

DOI: 10.1021/acs.jpclett.9b00619
J. Phys. Chem. Lett. 2019, 10, 2554−2560

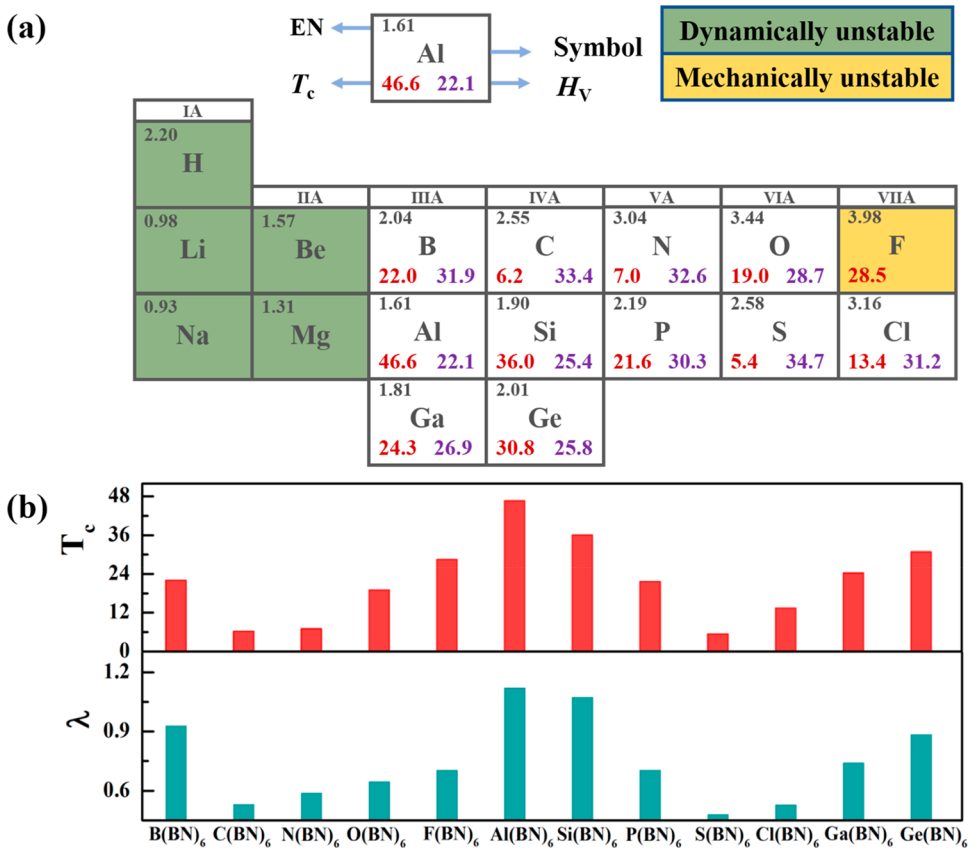

Figure 4. Superconductive and hard properties: (a) The detailed value of T_c and hardness (H_v) among all the predicted doped materials and the electronegativity (EN) of dopant on the Pauling scale. (b) The specific T_c (top panel) and the EPC parameter λ (bottom panel) of various doped compounds.

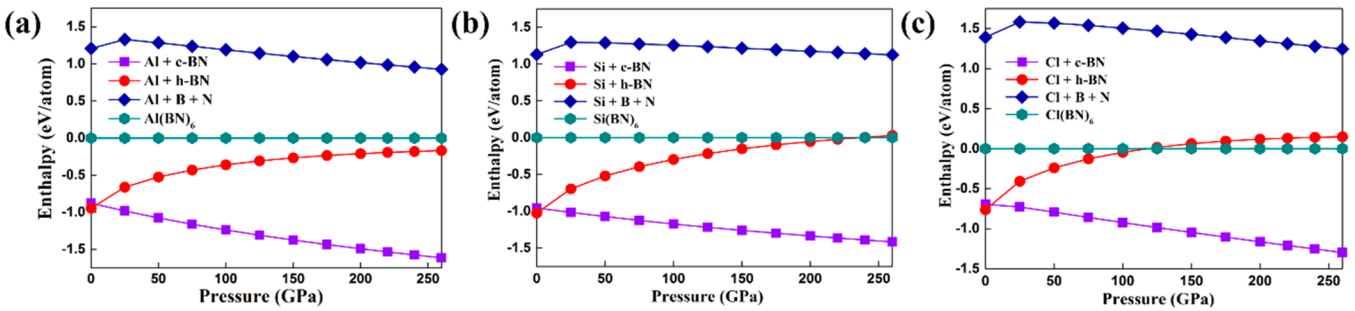

Figure 5. Calculated enthalpy for various structures as a function of pressure: (a) $Al(BN)_6$, (b) $Si(BN)_6$, and (c) $Cl(BN)_6$.

the lowest Pauling electronegativity and ionization energy among the dopants that give stable materials. When Al is inserted into the pure $(BN)_6$ cage, it can transfer more electrons to the N atoms than the other dopants, inducing a stronger EPC. It is plausible that $Al(BN)_6$ possesses the highest superconducting transition temperature among the doped materials that we considered here. We speculate that the dopants supply electrons to the host materials via the Fermi level entering the conduction bands in *n*-type doping, eventually turning the insulating $(BN)_6$ cage into a superconductor. Interestingly, we find that among the studied materials the T_c values of the systems with *n*-type dopants are higher than those with *p*-type dopants.

It is well-known that the hard and incompressible materials are usually insulators since all valence electrons contributed to covalent bonds. However, hard superconducting materials are desirable for some special applications. To find superconductors that are also hard, we evaluated the mechanical properties of our predicted doped materials. Hardness, namely the ability to resist plastic deformation from hydrostatic compression, tensile load, or shear, is strongly related to the bulk modulus and shear modulus. Therefore, we systematically investigated the specific Vickers hardness (H_v) using an empirical model.[22] The results in Figure 4 show that $Al(BN)_6$ is predicted to be a good superconductor and a hard material with a Vicker's hardness of ~30 GPa, along with other doped $X(BN)_6$ compounds.

In order to investigate the thermodynamically stability of the predicted structures, we have systematically examined the formation enthalpies at ambient conditions as well as under pressure. The enthalpy differences of several predicted structures are shown in Figure 5 at the pressures of 0−260

DOI: 10.1021/acs.jpclett.9b00619
J. Phys. Chem. Lett. 2019, 10, 2554−2560

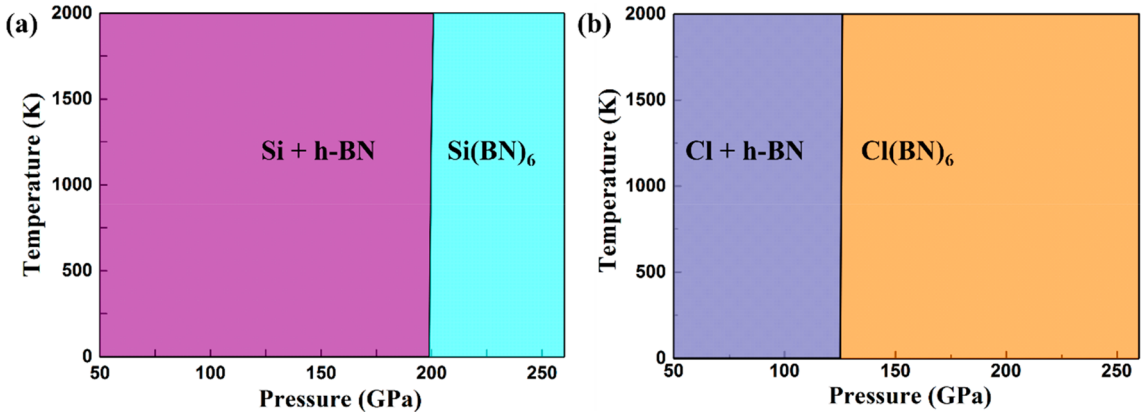

Figure 6. Pressure−temperature (P−T) phase diagram: The phase diagram of (a) $Si(BN)_6$ and (b) $Cl(BN)_6$.

GPa. It is clearly seen that the $X(BN)_6$ phases possess higher enthalpy than the BN compounds and metal elements, indicating they are metastable phases. Furthermore, we investigated the P-T phase diagram of several structures within the quasi-harmonic approximations (QHA), as shown in Figure 6. Remarkably, the $Si(BN)_6$ phase would be stable above 200 GPa at 1300 K, and the $Cl(BN)_6$ phase would be stable above 120 GPa at 0 K. Unfortunately, $Al(BN)_6$ remains unstable even at high pressure and high temperature. We should point out that our calculations did not consider all studied structures due to the expensively computational cost. However, we hope the current results will provide theoretical guidance for experiments in the future.

In summary, based on the mechanism of phonon-mediated superconductors, we predicted a new class of $(BN)_6$ sodalite-like cage materials that possess high T_c and favorable hardness. In particular, $Al(BN)_6$ has an exceptional T_c of 47 K at ambient pressure. It consists of unique $(BN)_6$ cage units and dopant atoms. Dense superconductive states, such as those reported here, may be favored in other mixtures of metals atoms and BN, possibly also upon compression. This work provides a key step in the exploration of high-T_c superconducting materials made of abundant elements, such as boron and nitrogen, under ambient conditions.

Ab initio structure optimizations were performed using density functional theory as implemented in the Quantum-espresso package.[23] Phonon dispersion and electron-EPC calculations were calculated within the framework of linear response theory through the Quantum-espresso code.[23] Among all the EPC calculations, the Ultrasoft pseudopotentials were selected with a kinetic energy cutoff of 45 Ry and a q-grid of 4 × 4 × 4 in the first BZ. K-grids of 16 × 16 × 16 were adopted to ensure k-point sampling convergence with a Methfessel-Paxton broadening width of 0.02 Ry to approximate the zero-width limit in the calculations of the EPC parameter, λ.

■ ASSOCIATED CONTENT

Supporting Information

The Supporting Information is available free of charge on the ACS Publications website at DOI: 10.1021/acs.jpclett.9b00619.

Phonon dispersion curves of $X(BN)_6$ (X = H, Li, Na, Be, Mg, B, C, N, O, F, P, S, Ga, Ge); relationship between charge transfer and atomic number; electronic band structures of $Al(BN)_6$ phases; relationship between T_c and bond length; formation energy against BN compounds and elements at ambient pressure; calculated T_c among predicted doped materials via different equations (PDF)

■ AUTHOR INFORMATION

Corresponding Authors

*S.L.: sylu2013@zzu.edu.cn.
*H.L.: hanyuliu@jlu.edu.cn.
*Y.L.: yinwei_li@jsnu.edu.cn.

ORCID

Xue Yong: 0000-0002-2134-7519
Min Wu: 0000-0001-5496-8066
Hanyu Liu: 0000-0003-2394-5421
Sheng Meng: 0000-0002-1553-1432

Author Contributions

▽X.L. and Y.X. equally contributed to this work.

Notes

The authors declare no competing financial interest.

■ ACKNOWLEDGMENTS

This work was supported by the National Natural Science Foundation of China (51373065, 91123031, 21221063, and 11722433). Part of the calculations have been performed by the use of computing resources provided by West Grid and Compute Canada. We acknowledge funding from Supported by NSAF (No. U1530124), the National Natural Science Foundation of China (Grant No. 11534003), Science Challenge Project No. TZ2016001, and Program for JLU Science and Technology Innovative Research Team (JLUSTIRT). Y.L. acknowledges funding from the Qing Lan Project and the Six Talent Peaks Project of Jiangsu Province. We utilized computing facilities at the High Performance Computing Center of Jilin University and Tianhe2-JK at the Beijing Computational Science Research Center.

■ REFERENCES

(1) Connétable, D.; Timoshevskii, V.; Masenelli, B.; Beille, J.; Marcus, J.; Barbara, B.; Saitta, A. M.; Rignanese, G. M.; Mélinon, P.; Yamanaka, S.; et al. Superconductivity in Doped sp^3 Semiconductors: the Case of the Clathrates. *Phys. Rev. Lett.* **2003**, *91*, 247001.

(2) Zipoli, F.; Bernasconi, M.; Benedek, G. Electron-Phonon Coupling in Halogen-doped Carbon Clathrates from First Principles. *Phys. Rev. B: Condens. Matter Mater. Phys.* **2006**, *74*, 205408.

DOI: 10.1021/acs.jpclett.9b00619
J. Phys. Chem. Lett. 2019, 10, 2554−2560

(3) Rey, N.; Alfonso, M.; Placida, R.-H.; Alfonso San, M. First-Principles Study of Lithium-doped Carbon Clathrates under Pressure. *J. Phys.: Condens. Matter* **2008**, *20*, 215218.
(4) Zeng, T.; Hoffmann, R.; Nesper, R.; Ashcroft, N. W.; Strobel, T. A.; Proserpio, D. M. Li-Filled, B-substituted Carbon Clathrates. *J. Am. Chem. Soc.* **2015**, *137*, 12639−12652.
(5) Paine, R. T.; Narula, C. K. Synthetic Routes to Boron Nitride. *Chem. Rev.* **1990**, *90*, 73−91.
(6) Sato, T.; Ishii, T.; Setaka, N. Formation of Cubic Boron Nitride from Rhombohedral Boron Nitride by Explosive Shock Compression. *J. Am. Ceram. Soc.* **1982**, *65*, c162−c162.
(7) Wentorf, R., Jr Cubic Form of Boron Nitride. *J. Chem. Phys.* **1957**, *26*, 956−956.
(8) Bundy, F. P.; Kasper, J. S. Hexagonal Diamond-a New Form of Carbon. *J. Chem. Phys.* **1967**, *46*, 3437−3446.
(9) Hamilton, E. J. M.; Dolan, S. E.; Mann, C. M.; Colijn, H. O.; McDonald, C. A.; Shore, S. G. Preparation of Amorphous Boron Nitride and Its Conversion to a Turbostratic, Tubular Form. *Science* **1993**, *260*, 659.
(10) Zhi, C.; Bando, Y.; Tang, C.; Golberg, D. Boron Nitride Nanotubes. *Mater. Sci. Eng., R* **2010**, *70*, 92−111.
(11) Corso, M.; Auwärter, W.; Muntwiler, M.; Tamai, A.; Greber, T.; Osterwalder, J. Boron Nitride Nanomesh. *Science* **2004**, *303*, 217.
(12) Kawaji, H.; Horie, H.; Yamanaka, S.; Ishikawa, M. Superconductivity in the Silicon Clathrate Compound $(Na,Ba)_xSi_{46}$. *Phys. Rev. Lett.* **1995**, *74*, 1427−1429.
(13) Tanigaki, K.; Shimizu, T.; Itoh, K. M.; Teraoka, J.; Moritomo, Y.; Yamanaka, S. Mechanism of Superconductivity in the Polyhedral-network Compound Ba_8Si_{46}. *Nat. Mater.* **2003**, *2*, 653.
(14) Ekimov, E. A.; Sidorov, V. A.; Bauer, E. D.; Mel'nik, N. N.; Curro, N. J.; Thompson, J. D.; Stishov, S. M. Superconductivity in Diamond. *Nature* **2004**, *428*, 542.
(15) Bustarret, E.; Marcenat, C.; Achatz, P.; Kačmarčik, J.; Lévy, F.; Huxley, A.; Ortéga, L.; Bourgeois, E.; Blase, X.; Débarre, D.; et al. Superconductivity in Doped Cubic Silicon. *Nature* **2006**, *444*, 465.
(16) Ren, Z.-A.; Kato, J.; Muranaka, T.; Akimitsu, J.; Kriener, M.; Maeno, Y. Superconductivity in Boron-Doped SiC. *J. Phys. Soc. Jpn.* **2007**, *76*, 103710.
(17) Kriener, M.; Maeno, Y.; Oguchi, T.; Ren, Z. A.; Kato, J.; Muranaka, T.; Akimitsu, J. Specific Heat and Electronic States of Superconducting Boron-Doped Silicon Carbide. *Phys. Rev. B: Condens. Matter Mater. Phys.* **2008**, *78*, 024517.
(18) Li, Y.; Feng, X.; Liu, H.; Hao, J.; Redfern, S. A. T.; Lei, W.; Liu, D.; Ma, Y. Route to High-energy Density Polymeric Nitrogen t-N via He-N Compounds. *Nat. Commun.* **2018**, *9*, 722.
(19) Li, Y.; Hao, J.; Liu, H.; Lu, S.; Tse, J. S. High-Energy Density and Superhard Nitrogen-Rich B-N Compounds. *Phys. Rev. Lett.* **2015**, *115*, 105502.
(20) Bardeen, J.; Cooper, L. N.; Schrieffer, J. R. Microscopic Theory of Superconductivity. *Phys. Rev.* **1957**, *106*, 162−164.
(21) Lu, S.; Liu, H.; Naumov, I. I.; Meng, S.; Li, Y.; John, S. T.; Yang, B.; Hemley, R. J. Superconductivity in Dense Carbon-based Materials. *Phys. Rev. B: Condens. Matter Mater. Phys.* **2016**, *93*, 104509.
(22) Tse, J. S. Intrinsic Hardness of Crystalline Solids. *J. Super. Mater.* **2010**, *32*, 177−191.
(23) Giannozzi, P.; Stefano, B.; Nicola, B.; Matteo, C.; Roberto, C.; Carlo, C.; Davide, C.; Guido, L. C.; Matteo, C.; Ismaila, D.; et al. Quantum Espresso: a Modular and Open-Source Software Project for Quantum Simulations of Materials. *J. Phys.: Condens. Matter* **2009**, *21*, 395502.

DOI: 10.1021/acs.jpclett.9b00619
J. Phys. Chem. Lett. 2019, 10, 2554−2560